

QUANTIFICATION OF OCTUPOLE MAGNETS AT THE UNIVERSITY OF MARYLAND ELECTRON RING*

H. Baumgartner[†], S. Bernal, I. Haber, T. Koeth, D. Matthew, K. Ruisard, M. Teperman,
B. Beaudoin, University of Maryland, College Park, USA

Abstract

It is particularly important to manage beam loss in high intensity accelerators, because the large beam current can result in heating, damage, and activation of components. A lattice of strong nonlinear magnets is predicted by theory to damp resonances while maintaining dynamic aperture. Results of rotating coil measurements and magnetic field scans will be presented, quantifying the multipole moments and fringe fields of PCB octupoles in UMER's nonlinear lattice experiments.

INTRODUCTION

The University of Maryland Electron Ring (UMER) is a 10 keV, 11.52 meter electron ring for the study of intense beam dynamics. UMER is embarking on a new effort to investigate integrable nonlinear optics, which is a promising area of research in high-intensity ring design [1]. To this end, a quasi-integrable octupole lattice will be incorporated into the existing FODO ring structure [2]. Currently, the entire UMER ring utilizes air-core dipole and quadrupole magnets constructed from flexible printed circuits (Fig. 1). These PCBs are inexpensive to manufacture and can be made with a quick turnaround time. The 2oz copper thickness can easily sustain currents of 2A with no additional cooling, or up to 10A with water cooling. The thin profile of the flexible PCB opens up the possibility of stacking multiple PCBs into one mount, or even utilizing the multi-layer capabilities of circuit board manufacturing to make a single PCB with different magnets on different PCB layers.

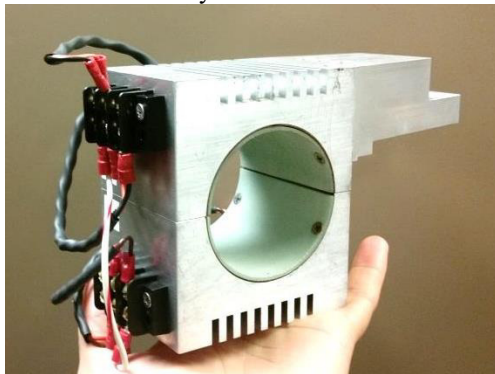


Figure 1: Assembled PCB magnet showing the aluminium housing and G10 liner. The flex PCB is underneath the liner. The magnet length is 2.3" and the bore diameter is 2.2".

A magnet is comprised of two PCBs that form its top and bottom half. Each magnet half is mounted into an aluminum housing, aligned with pins and held in place with a formed G10 liner. The two halves of the magnet are then placed around the beam pipe and bolted together.

Recently, octupole PCB magnets were designed for the UMER nonlinear optics project [3]. This paper presents the results of numerical calculations and empirical measurements of the PCB octupole magnets.

MAGNET DESIGN

The magnetic multipole expansion is given by [4] is

$$B_y + iB_x = \sum_{n=1} (b_n + ia_n) \left(\frac{x+iy}{r_0} \right)^{n-1} \quad (1)$$

Multipoles can be created by an angularly dependent current distribution given by Eq. 2 [4], where z is the longitudinal coordinate, a is an adjustable parameter, L is magnet length and n is the pole order.

$$\sin(n\theta) = 1 - \left(\frac{2z}{aL} \right)^2 \quad (2)$$

In the UMER PCB magnets, this azimuthally varying current distribution is achieved by creating spiral traces of varying density and length, as shown in Figure 2. Conductors parallel to the beam axis, forming the diamond shape, contribute to the field, while conductors perpendicular to the beam axis are simply return traces.

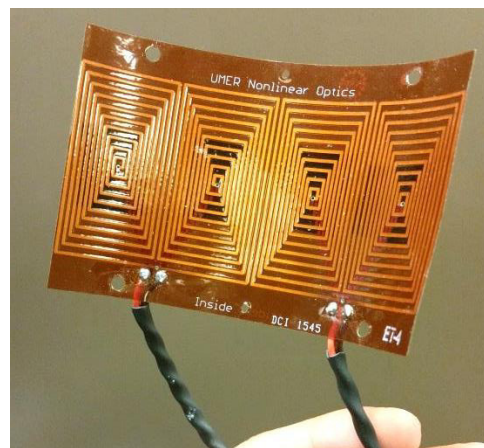


Figure 2: The flex PCB containing the windings of the octupole magnet.

Because of the small aspect ratio of these magnets, they are dominated by fringe fields. As such, it is especially important to characterize the magnet with good longitudinal resolution.

* Supported by DOE-HEP and the NSF Accelerator Science Program.

[†] heidib@umd.edu

MEASUREMENT TECHNIQUES

Gauss Probe Measurement

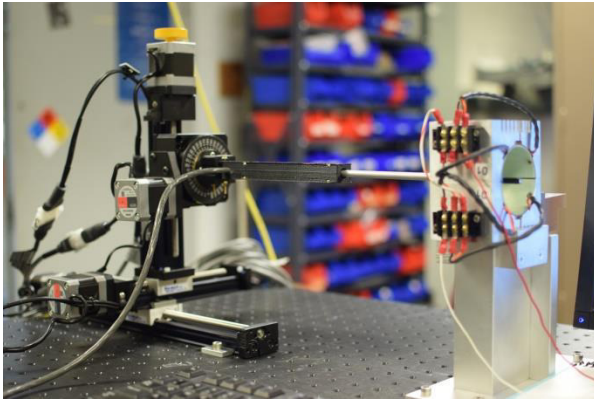


Figure 3: Gauss probe setup.

A Gauss probe allows for precise local measurements of magnetic field. We used a Lake Shore Model 460 3-channel Gauss meter with a MMZ-2508-UH 3-axis probe mounted to a Velmex stage with 3 axes of travel as well as one rotation axis. The setup was not shielded from background magnetic fields, but the probe's position between trials could be reproduced to within thousandths of an inch, so separate measurement and background scans were done each time.

It was a particular challenge to mount the Gauss probe to the stage, due to its unwieldy length and lack of mounting holes. To mount the probe to the stage, a 3D-printed holder was designed, which clamped the probe tightly in place (see Figure 3). The center of the probe was aligned with the center of the rotation stage, and rotary scan was done by translating the probe as well as rotating it. To compensate for skew of the probe, the travel of the probe during rotations was observed using a camera, and the offset of the probe tip from the base was calculated from captured images.

We allowed a 1-second settling time after every movement before a measurement to allow any vibrations in the probe tip to dissipate. As a result, a full radial scan with sufficient data points to draw a smooth plot took several minutes. Unlike the rotating coil, where the FFT is taken in real-time, adjustments to a Gauss probe setup are quite slow.

Magnetic center was found by scanning linearly across the bore in the center of the magnet and finding the zero field point. Steps of 0.03" were not sufficient resolution and required further manual adjustment based on the shape of the radial plot.

Rotating Coil Measurement

The rotating coil measurements were made with a transverse coil well exceeding the length of the magnet, comprised of about 3000 turns of AWG 44 wire. The coil rotates at 6 Hz and the induced current through the coil is measured as a voltage across a terminating resistor with the use of an oscilloscope, capable of computing a real-time FFT.

Adjustment of the magnet's position was done using three micrometer screws. The screws are adjusted to maximize the octupole component while minimizing the lower order components, watching the spectrum on the oscilloscope. After this adjustment is done, the setup is shielded with a mu metal box. A background scan is also performed before collecting data.

MAG-LI Simulations

MAG-LI is a Biot-Savart solver written by former UMER graduate student Hui Li. It models the circuit board as a set of infinitely thin wires.

RESULTS

Rotating Coil

The rotating coil displays a prominent octupole peak, and quite small lower order peaks. The mu metal shielding of the rotating coil setup was effective at reducing the Earth's magnetic field, and the easy alignment procedure to position the rotating coil at the center of the octupole ensured a small quadrupole peak, as shown in Fig. 4.

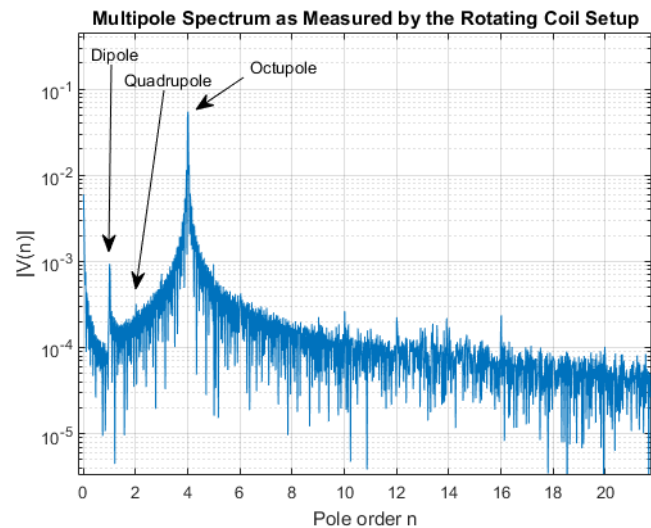


Figure 4: Frequency spectrum of rotating coil measurement at 2A. Octupole, quadrupole and dipole peaks at $n=4$, 2 and 1 respectively, are indicated by arrows.

Gauss Probe

XY Scan

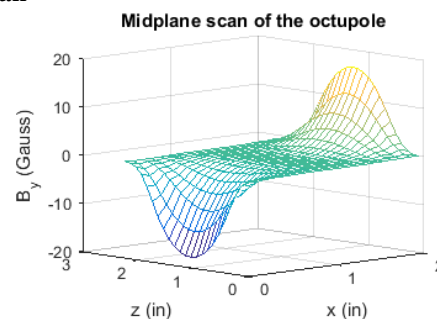


Figure 5: Gauss probe measurement at 2.5A of the midplane of the octupole spanning the entire magnet bore.

The Gauss probe gives us the ability to create a raster scan of any desired surface or volume inside the bore of the magnet. A raster scan of the midplane shows the transverse x^3 profile of the magnetic field's y-component, as well as the longitudinal profile. From a scan across the midplane we have determined the octupole gradient of $51.6 \pm 1.5 \text{ T/m}^3/\text{A}$. See Figure 5.

Radial Scan

$|B_\theta|$ (Gauss) at a variety of longitudinal positions, measured

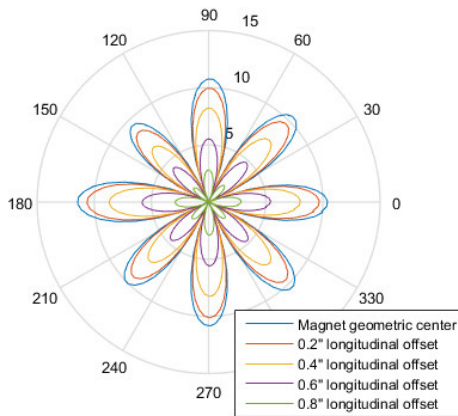


Figure 6: Polar plots of radial magnetic field from Gauss probe scans at 0.8” radii (73% of bore radius) at various longitudinal positions.

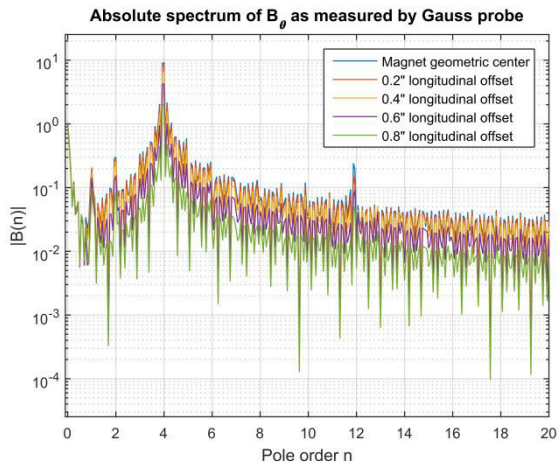


Figure 7: Multipole spectrum derived from the above radial data measured using a Gauss probe.

Figures 6 and 7 display data from multiple radial scans using the Gauss probe, starting at the geometric center of the magnet and moving in the z direction towards the edge in 0.2” increments. Effort was made to do the scan as close as possible to the aperture of the bore, because measurement errors decrease exponentially away from the boundary.

Prominent quadrupole and dipole peaks are present, indicating that the radial scan was done off-center. Furthermore, there is a strong peak at $n=12$, though no peak is present at $n=16$ as there was in the rotating coil measurement.

Simulation

$|B_\theta|$ (Gauss) from MAG-LI at a variety of longitudinal positions

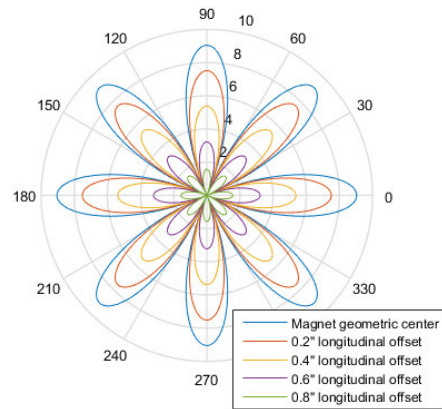


Figure 8: Polar plots of radial magnetic field from MAG-LI at 0.8” radii at various longitudinal positions.

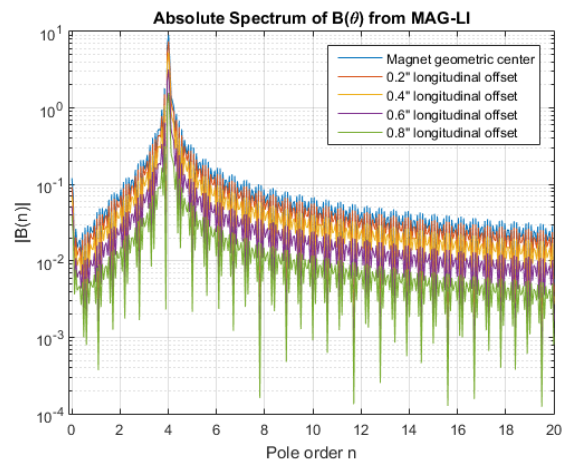


Figure 9: Multipole spectrum derived from the above MAG-LI radial data.

Finally, Figures 8 and 9 are the same FFT spectra and polar plots as the prior two figures, obtained from simulation with Mag-LI. They show an agreement of the general features of the data and suggest no flaws in the magnet as designed, which calls for further investigation of whether the empirical measurements show true design flaws or require further refinement in the data collection technique or magnet assembly.

ACKNOWLEDGMENT

Thanks to the rest of UMER group for their technical support and invaluable insight: Rami Kishek, Dave Sutter, Moiz Siddiqi, Levon Dovlatyan.

REFERENCES

- [1] Danilov, V., Nagaitsev, S., Nonlinear accelerator lattices with one and two analytic invariants. Phys. Rev. ST Accel. Beams 13:084002 (2010).
- [2] K. Ruisard *et al.*, "Early Results and Experimental Plans for Single-Channel Strong Octupole Fields at the University of Maryland Electron Ring", these proceedings.

- [3] Matthew, D., Improved UMER Magnet Design Process. Technical Note (Unpublished), 31 August, 2015.
- [4] W.W. Zhang, *et al.*, Design and field measurement of printed-circuit quadrupoles and dipoles, Physical Review, Special Topics – Accel Beams 3, 122401 (2000).